BIOCHEMISTRY
including biophysical chemistry & molecular biology

ARTICLE

pubs.acs.org/biochemistry

Partitioning of Synaptotagmin I C2 Domains between Liquid-Ordered and Liquid-Disordered Inner Leaflet Lipid Phases

Chen Wan,[†,‡] Volker Kiessling,[†,‡] David S. Cafiso,[†,§] and Lukas K. Tamm*[,†,‡]

[†]Center for Membrane Biology, [‡]Department of Molecular Physiology and Biological Physics, and [§]Department of Chemistry, University of Virginia, Snyder Building, P.O. Box 800886, Charlottesville, Virginia 22908, United States

Supporting Information

ABSTRACT: Synaptotagmin I is the calcium sensor in synchronous neurotransmitter release caused by fusion of synaptic vesicles with the presynaptic membrane in neurons. Synaptotagmin I interacts with acidic phospholipids, but also with soluble *N*-ethylmaleimide-sensitive factor attachment receptors (SNAREs), at various stages in presynaptic membrane fusion. Because SNAREs can be organized into small cholesterol-dependent clusters in membranes, it is important to determine whether the C2 domains of synaptotagmin target membrane domains with different cholesterol contents. To address this question, we used a previously developed asymmetric two-phase lipid bilayer system to investigate the membrane binding and lipid phase targeting of soluble C2A and C2AB domains of synaptotagmin. We found that both domains target more disordered cholesterol-poor domains better than highly ordered cholesterol-rich domains. The selectivity is greatest (~3-fold) for C2A binding to disordered domains that are formed in the presence of 5 mol % PIP_2 and 15 mol % PS. It is smallest (~1.4-fold) for C2AB binding to disordered domains that are formed in the presence of 40 mol % PS. In the course of these experiments, we also found that C2A domains in the presence of Ca^{2+} and C2AB domains in the absence of Ca^{2+} are quite reliable reporters of the acidic lipid distribution between ordered and disordered lipid phases. Accordingly, PS prefers the liquid-disordered phase over the liquid-ordered phase by ~2-fold, but PIP_2 has an up to 3-fold preference for the liquid-disordered phase.

Ca^{2+}-triggered membrane fusion of synaptic vesicles with the presynaptic plasma membrane of neurons is the central event in synaptic transmission. This process is tightly regulated by synaptotagmin I (syt I), soluble *N*-ethylmaleimide-sensitive factor attachment receptor (SNARE) proteins, and other factors.[1−3] Assembly of the four-helix bundle SNARE protein complex docks the vesicles to the presynaptic membrane and is believed to be the essential reaction that drives membrane fusion.[4−8] syt I is an integral membrane protein of synaptic vesicles and is the Ca^{2+} sensor for synchronous neurotransmitter release.[9−13] It is anchored to the membrane by a single transmembrane domain near the N-terminus and contains two C2-type Ca^{2+}-sensing domains (C2A and C2B) toward its C-terminal end.[14] A long linker connects C2A to the TM domain, and a short linker connects C2A and C2B. C2A and C2B have similar folds consisting of a β-sandwich formed from two four-strand β-sheets. The loops that connect the β-strands protruding from one end form binding sites for Ca^{2+} ions, binding three or two Ca^{2+} ions, respectively. Ca^{2+} bound to these loops mediates the binding of C2 domains to negatively charged membrane surfaces.[15,16] In general, syt I C2 domains can interact with the synaptic vesicle membrane (cismembrane) as well as with the presynaptic plasma membrane (transmembrane).[17] In the following, we will only consider the transmembrane interactions that are independent of the TM domain, which resides in the cismembrane.

The C2 domains of syt I have been proposed to regulate fusion through interaction with acidic phospholipids such as phosphatidylserine (PS) and phosphatidylinositol (PI) and its phosphorylated derivatives by binding and penetrating into the presynaptic membrane surface upon Ca^{2+} binding.[18−20] In fact, when expressed as independent domains, the two C2 domains have been reported to prefer different membrane compositions. The membrane binding of C2A and C2B is strongly dependent on Ca^{2+}, and they bind well to bilayers composed of negatively charged lipids. However, C2A has a preference for PC/PE bilayers containing PS while C2B prefers to bind to bilayers containing PIP_2. C2B even binds weakly in the absence of Ca^{2+} to PC/PE/PS or PC/PE/PIP_2 bilayers through a highly basic strand in its β-sandwich.[21−23] When expressed as tandem C2A and C2B domains, the two domains reinforce each other's binding and membrane penetration behavior.[24] Expressed C2A and C2B have also been reported to change membrane curvature,[25] and full-length syt I co-reconstituted with SNAREs can enhance SNARE-mediated fusion under appropriate conditions.[26,27] However, exactly how syt I cooperates with SNAREs and thereby imparts Ca^{2+} control on neuronal exocytosis is not yet fully understood.

The SNAREs syntaxin 1A and SNAP-25 are concentrated in partially overlapping clusters in plasma membranes that are also the sites of exocytosis in neuroendocrine cells[28] and pancreatic β cells.[29] Cholesterol depletion disperses these clusters in plasma membranes and simultaneously impairs exocytosis. Although these clusters are cholesterol-dependent, SNAREs are not found in detergent-resistant fractions and, therefore, are unlikely targeted to "rafts" in cell membranes. These results raise the question of whether syt I C2 domains prefer cholesterol-rich or cholesterol-poor regions of the plasma membrane and whether regulation of such partitioning could regulate potential interactions with SNAREs. Because C2 domains target the

Received: November 22, 2010
Revised: January 21, 2011
Published: February 15, 2011

cytoplasmic (inner) leaflets of plasma and intracellular membranes, one strategy for answering this question is to use model membranes with coexisting liquid-ordered (l_o) and liquid-disordered (l_d) domains and inner leaflet lipid compositions. Unlike mixtures of PC, SM, and cholesterol, typical inner leaflet lipid mixtures of PC, PE, PS, and cholesterol do not form phase-separated l_o and l_d phases on their own in model membranes.[30,31] However, such domains can be induced to form by phase coupling adjacent to phase-separated l_o−l_d domains formed by outer leaflet lipid PC, SM, and cholesterol mixtures in asymmetric supported lipid bilayers.[30,32]

In this work, we investigate the Ca^{2+}-dependent binding and surface distribution of syt I C2A and C2AB on asymmetric bilayers with induced coexisting l_o−l_d phases, as well as the Ca^{2+}-independent binding of C2AB on these bilayers as a function of the concentrations of the anionic lipids PS and PIP_2 and the curvature-inducing lipid PE in the inner leaflet. We find that under all lipid conditions, C2 domains favor l_d over l_o lipid phases in the presence and absence of Ca^{2+}. C2A's binding preference for l_d phases is independent of the PS concentration, probably reflecting a concentration-independent partitioning of this lipid between ordered and disordered phases. However, C2A partitioning between l_o and l_d lipid phases depends on the PIP_2 concentration, indicating a progressively higher level of accumulation of PIP_2 in disordered membrane regions as PIP_2 and C2A levels are increased. The selectivity of C2AB for disordered membrane regions is not as high as that of C2A, and importantly, C2AB in the absence of Ca^{2+} can be used as a reliable reporter of acidic lipid partitioning between inner leaflet l_d and l_o phases in asymmetric lipid bilayers.

MATERIALS AND METHODS

The following materials were purchased and used without further purification: POPS, bPC, bSM, bPE, $bPIP_2$, NBD-DPPE, and Rh-DPPE (Avanti Polar Lipids, Alabaster, AL); Alexa Fluor 546 C_5-maleimide (Invitrogen, Carlsbad, CA); cholesterol, HEPES, and glycerol (Sigma Chemical Co., St. Louis, MO); and chloroform, ethanol, methanol, ether, Contrad detergent, all inorganic salts, acids, bases, and hydrogen peroxide (Fisher Scientific, Fair Lawn, NJ). DPS was custom synthesized by Shearwater Polymers (Huntsville, AL). Water was purified first with deionizing and organic-free filters (Virginia Water Systems, Richmond, VA) and then with a NANOpure system from Barnstead (Dubuque, IA) to achieve a resistivity of 18.2 MΩ/cm. The following buffers were used for vesicle preparation and protein binding: HKE buffer [25 mM HEPES, 100 mM KCl, and 1 mM EGTA (pH 7.4)] and HKC buffer [25 mM HEPES, 100 mM KCl, and 1 mM $CaCl_2$ (pH 7.4)]. Synaptotagmin I C2A and C2AB lacking the transmembrane domains were prepared as described previously.[19,33]

Large Unilamellar Vesicles (LUVs). The desired lipids were codissolved in chloroform or a chloroform/methanol mixture. Solvent was evaporated under a stream of N_2 gas, using a rotary evaporator when PIP_2 was present. After the sample had been dried for 1 h in vacuum, the resulting residue was suspended in HKE buffer, rapidly vortexed, frozen and thawed five times by alternate submersion in liquid N_2 and then a water bath at 40 °C, and then extruded by 15 passes through two polycarbonate membranes with a pore diameter of 100 nm (Avestin, Ottawa, ON). Vesicles were stored at 4 °C for not more than 5 days before use.

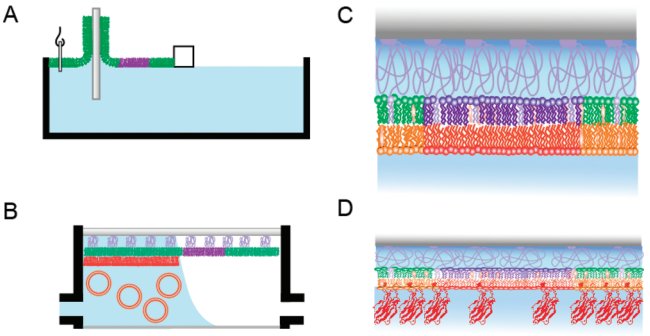

Figure 1. Preparation of asymmetric two-phase supported bilayers and protein binding. (A) Langmiur−Blodgett (LB) film deposition. The bPC/bSM/cholesterol/polymer lipid mixture was spread on the air−water interface and compressed to form a lipid monolayer. The quartz substrate was rapidly dipped and slowly raised through this interface. A constant surface pressure was maintained through computer feedback during this process. (B) Vesicle fusion (VF). The LB-coated quartz slide was placed in a custom-built flow-through chamber. A LUV solution was slowly and carefully injected into the chamber and allowed to spontaneously fuse with the LB monolayer. Excess vesicles were then washed out by extensive buffer rinsing. (C) Single planar polymer-supported bilayer formed from l_o phase-inducing lipid combinations in panels A and B. (D) Binding of synaptotagmin I C2A or C2AB domains after perfusion and washing of the chamber with a preformed asymmetric bilayer.

Quartz Slides. Slides (40 mm × 25 mm × 1 mm) were purchased from Quartz Scientific (Fairport Harbor, OH). They were cleaned by being boiled in Contrad detergent for 10 min and then sonicated while still in detergent for 30 min, followed by extensive rinsing with water, methanol, and water again. Remaining organic residues were removed by immersion in 3 volumes of sulfuric acid to 1 volume of 30% hydrogen peroxide, followed by extensive rinsing in water. Immediately prior to use, slides were further cleaned for 10 min in an argon plasma sterilizer (Harrick Scientific, Ossining, NY).

Tethered Polymer-Supported Bilayers. The bilayers were formed as illustrated in Figure 1 by a combined Langmuir−Blodgett/vesicle fusion (LB/VF) technique.[34−36] A lipid monolayer containing 3% DPS was spread from a chloroform solution onto a pure water surface in a Nima 611 Langmuir−Blodgett trough (Nima, Conventry, U.K.). The solvent was allowed to evaporate for 10 min, and the monolayer was compressed at a rate of 10 cm^2/min to reach a surface pressure of 32 mN/m and equilibrated for 5−10 min. A clean quartz slide was then rapidly (200 mm/min) dipped into the trough and slowly (5 mm/min) withdrawn, while a feedback circuit maintained a constant surface pressure and monitored the transfer of lipids onto the substrate by measuring the change in surface area. The resulting monolayer on the solid support is known as the LB monolayer. The DPS molecules were tethered to the surface by drying the coated slides in a desiccator at room temperature overnight and subsequently curing them in a 70 °C oven for 40 min. The slide was transferred to a desiccator, allowed to equilibrate at room temperature, and typically used on the same day.

Slides with tethered polymer-supported LB monolayers were placed in a custom-built flow-through chamber. A 0.1 mM suspension of large unilamellar vesicles in HKE buffer was slowly and carefully injected into the chamber to prevent the LB monolayer from being washed away and then incubated for 35 min. Excess vesicles were washed out by extensive rinsing with HKE

buffer. Inner leaflet monolayers containing 40% POPS required 1 mM $CaCl_2$ during vesicle fusion for reproducible bilayer formation.

Fluorescence Labeling of Synaptotagmin I C2 Domains. Both synaptotagmin I C2A and C2AB domains used in this study had single-cysteine mutations (syt I C2A L142C and syt I C2AB E269C) for labeling with Alexa Fluor 546. The labeled cysteine residues are exposed to the aqueous environment far from the membrane binding loops.[19,33] We therefore do not expect fluorophores to insert into the lipid bilayer and thereby change their intensity. Syt I C2 domains were dissolved in a degassed 10 mM HEPES buffer (pH 7.0); a 10-fold molar excess of tris(2-carboxylethyl)phosphine (TCEP) was added, and the solution was incubated at room temperature for 2 h. Alexa Fluor 546 at 1 mg/mL [10 mM HEPES (pH 7.4)] was added to yield a dye:protein molar ratio of 10:1 and the mixture incubated at 4 °C overnight. Unreacted dyes were removed by Sephadex G-50 gel filtration in 10 mM HEPES buffer (pH 7.0). Labeling efficiencies between 30 and 90% were obtained as determined by absorbance spectroscopy using the extinction coefficient of Alexa Fluor 546 (93000 M^{-1} cm^{-1}).

Epifluorescence Microscopy. Images were recorded on a Zeiss Axiovert 200 fluorescence microscope (Carl Zeiss, Thornwood, NY) with a mercury lamp as a light source, a 63× water immersion objective (Carl Zeiss; NA = 0.95), and an electron multiplying charge-coupled device (EMCCD) cooled to −70 °C (iXon DV887ESC-BV, Andor, Belfast, U.K.) as a detector. Images were acquired using homemade software written in LabVIEW (National Instruments, Austin, TX). Bilayers stained with NBD-DPPE were illuminated through a 480 nm band-pass filter (D480/30, Chroma, Brattleboro, VT) and via a dichroic mirror (505dclp, Chroma) through the objective. Fluorescence was observed through a 535 nm band-pass filter (D535/40, Chroma). Alexa Fluor 546 C5-maleimide-labeled protein layers were illuminated through a 540 nm band-pass filter (D540/25, Chroma) and via a dichroic mirror (565dclp, Chroma) through the objective. Fluorescence was observed through a 605 nm band-pass filter (D605/55, Chroma).

Total Internal Reflection Fluorescence Microscopy (TIRFM). A Zeiss Axiovert 35 fluorescence microscope (Carl Zeiss) with an argon ion laser beam (Innova 300C, Coherent, Palo Alto, CA) as a light source and a 40× water immersion objective (Carl Zeiss; NA = 0.75) was used for TIRFM. Fluorescence images (128 pixels × 128 pixels) were recorded through a 610 nm band-pass filter (D610/60, Chroma) by an EMCCD cooled to −70 °C (iXon DU-860E-CSO-#BV, Andor) and acquired using homemade software written in LabVIEW (National Instruments). To monitor the Alexa Fluor 546-labeled protein layer, the focused laser beam was tuned to 514 nm and directed through a trapezoidal prism onto the quartz−buffer interface where the supported bilayer was attached. The prism−quartz interface was lubricated with glycerol to allow easy translocation of the sample chamber on the microscope stage. The laser beam was totally internally reflected at an angle of 72° from the surface normal, producing an evanescent wave that decays exponentially in the solution with a characteristic penetration depth of ∼100 nm in our setup. An elliptical area of ∼250 μm × ∼65 μm was illuminated and observed. The intensity of the laser beam was computer-controlled through an acousto-optic modulator (AOM-40, IntraAction, Bellwood, IL) or could be completely blocked by a computer-controlled shutter (Vincent Associates, Rochester, NY).

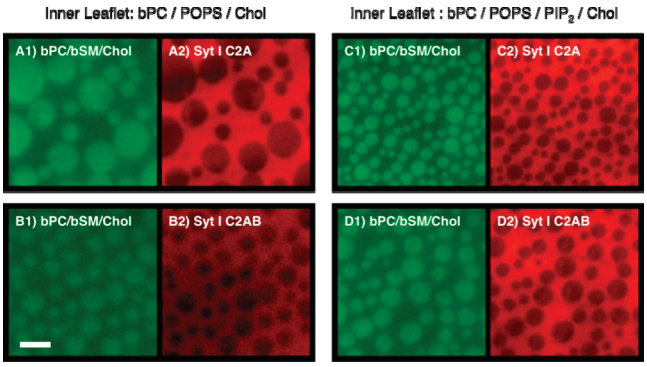

Figure 2. Representative images of Ca^{2+}-mediated synaptotagmin I C2A and C2AB domains binding to asymmetric two-phase bilayers with bPC/bSM (1:1) outer leaflet monolayers that include 20% cholesterol and are supported on a polymer cushion and inner leaflet monolayers composed of bPC, 15% POPS, and 20% cholesterol (left) or bPC, 15% POPS, 1% $bPIP_2$, and 20% cholesterol (right). The outer leaflet monolayers are visualized with 0.25% NBD-DPPE, which preferentially partitions into l_o phases (green images). The inner leaflet monolayers are not labeled but are known to form induced l_o phases on top of outer leaflet l_o phases.[30] Alexa Fluor 546-labeled synaptotagmin I C2A (top) and C2AB (bottom) domains bind to induced inner leaflet l_o and l_d phase domains and preferentially partition to the more disordered lipid phase regions (red images). The scale bar is 10 μm.

Binding of Synaptotagmin I C2 Domains to Supported Bilayers. Two milliliters of a 0.2 μM Alexa Fluor 546-labeled syt I C2 domain solution (HKE or HKC buffer) was injected into the flow-through chamber containing an asymmetric supported bilayer. The binding process was monitored for 15−20 min by TIRFM, and the images were recorded every 30 s. Multiple images from surrounding areas were taken after binding was completed. Excess protein was washed away by 10 volumes of HKE or HKC buffer. Polarized TIRFM[37,38] experiments revealed that the fluorescence intensities from different phases are proportional to the amount of protein binding. Comparing images acquired under s- and p-polarized excitation light showed that the influence of the fluorophore orientation can be neglected (data not shown).

Image Analysis. Images of the protein layer were analyzed by homemade programs written in LabVIEW (National Instruments). The mean intensities from domain regions and nondomain regions were extracted separately, and the binding curves of those regions were reconstructed. The intensity ratios of domain over nondomain regions were calculated from the extracted intensities of domain and adjacent nondomain regions. Typically, 10−20 ratios were obtained for each image, and 10−30 images were taken for each condition after binding had reached saturation. The mean ratios, standard deviations, and standard errors (the standard deviations of the mean) were then calculated accordingly.

RESULTS

Synaptotagmin I C2A and C2AB Preferentially Bind to Liquid-Disordered Phase Regions on Asymmetric Two-Phase Lipid Bilayers. The preparation and geometry of asymmetric supported membranes are illustrated in Figure 1. The images in Figure 2 represent the outer leaflet [bPC/bSM (1:1) with 20% cholesterol] monolayers (green images) containing coexisting l_o and l_d phases and the bound C2 domain proteins

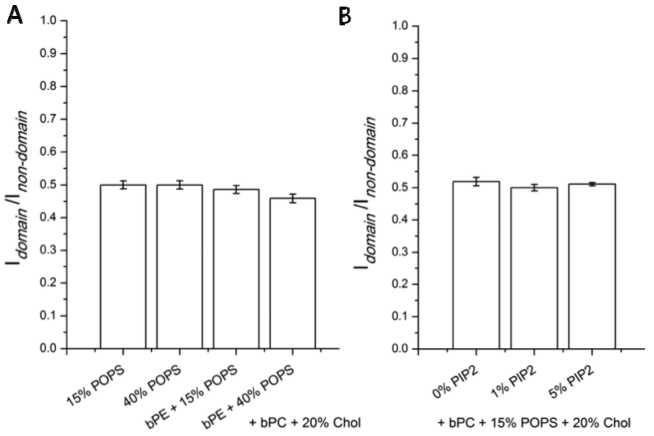

Figure 3. Synaptotagmin I C2AB fluorescence intensity ratios of ordered lipid domain regions over disordered lipid nondomain regions after binding to asymmetric two-phase bilayers in the absence of Ca^{2+} (1 mM EGTA). The lipid compositions of the inner leaflet monolayers are as labeled on the *x*-axis. All outer leaflet monolayers are composed of bPC and bSM (1:1) with 20% cholesterol and supported on a polymer cushion. (A) Fluorescence intensity ratios after binding to inner leaflet monolayers with different concentrations of PS and PE. The bPC:bPE ratio is 1:1 when bPE is present. (B) Fluorescence intensity ratios after binding to inner leaflet monolayers with different concentrations of PIP_2 in the presence of 15% PS. Error bars indicate standard errors.

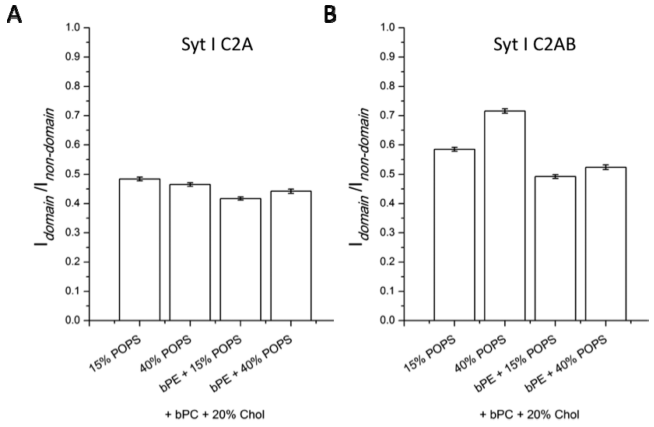

Figure 4. Synaptotagmin I C2A (A) and C2AB (B) fluorescence intensity ratios of ordered lipid domain regions to disordered lipid nondomain regions after binding to asymmetric two-phase bilayers in the presence of 1 mM Ca^{2+}. The inner leaflet monolayers contain different concentrations of PS and PE as indicated on the *x*-axis. The bPC:bPE ratio is 1:1 when bPE is present. All outer leaflet monolayers are composed of bPC and bSM (1:1) with 20% cholesterol and supported on a polymer cushion. Error bars indicate standard errors.

(red images) after binding to the inner leaflet of the asymmetric lipid bilayers. By convention, "outer" and "inner" refer in this study to the lipid leaflets of a cell plasma membrane that our asymmetric supported bilayers are mimicking and not to the configuration in the supported membrane. The outer leaflet lipid mixtures formed stable l_o and l_d phases as visualized by the lipid probe NBD-DPPE, which preferentially partitions into l_o phases.[39] The inner leaflet lipid mixtures contain either bPC, 15% POPS, and 20% cholesterol (Figure 2A,B) or bPC, 15% POPS, 20% cholesterol, and 1% $bPIP_2$ (Figure 2C,D).[a] The inner leaflet monolayers were not stained in these experiments but are known to form induced l_o phases on top of outer leaflet l_o phases through transbilayer phase coupling[30] (also see Supporting Information, for an example).

A solution containing 0.2 μM syt I C2A (Figure 2, panels A2 and C2) or C2AB (Figure 2, panels B2 and D2) in HKC buffer [25 mM HEPES, 100 mM KCl, and 1 mM $CaCl_2$ (pH 7.4)] was injected into the sample chamber to saturate the whole bilayer area. The binding process was monitored by TIRFM, and the protein images were taken 20−30 min after injection. The C2A and C2AB images are reversed in contrast when compared to the NBD-DPPE images of the outer leaflet monolayers. Therefore, both C2A and C2AB bind to inner leaflet monolayers preferentially in the more disordered lipid phase regions. This selective binding of C2A and C2AB was observed for all inner leaflet lipid mixtures that were investigated in this study, but the binding ratios varied depending on the conditions as described further below.

Calcium-Independent Binding of Synaptotagmin I C2AB. In the absence of Ca^{2+}, syt I C2A does not bind to any of these asymmetric bilayers containing anionic phospholipids. In marked contrast, syt I C2AB binds to such asymmetric bilayers in the absence of Ca^{2+} most likely through the interaction of the polybasic region of C2B with the anionic phospholipids.[21] Although we performed most of the experiments of this study as described above for Figure 2, no lipid dyes were included in the bilayers for the ratiometric experiments described below. We found that this refinement yielded more accurate protein binding ratios because it required no correction for bleed-through from NBD-DPPE fluorescence in the 540 nm channel.

Figure 3 shows the syt I C2AB fluorescence intensity ratios of l_o domain regions over l_d nondomain regions after binding to asymmetric planar supported lipid bilayers in the absence of Ca^{2+} (1 mM EGTA). The outer leaflets of these experiments contained bPC and bSM (1:1) with 20% cholesterol. The inner leaflets contained either bPC and 20% cholesterol with different concentrations of POPS with or without bPE (1:1 bPC:bPE ratio) (Figure 3A) or bPC, 15% POPS, and 20% cholesterol with different concentrations of $bPIP_2$ (Figure 3B). The mean fluorescence intensity ratios were ~0.5 and did not significantly depend on inner leaflet lipid compositions. It has been shown that when the polybasic region of C2B interacts electrostatically with anionic phospholipids in the absence of Ca^{2+}, it does not penetrate into the membrane.[21] This means that the calcium-independent binding of syt I C2AB depends on the charge density on the inner leaflet lipid surface and is less sensitive to specific lipid compositions. Therefore and assuming that the valence on the protein is not changed by the different lipid phases, our results show that the charge density on the l_d phase areas is significantly higher than that on the l_o phase areas. Figure 3 also indicates that the overall charge distribution between the l_o and l_d phases does not depend on the specific acidic lipid PS and PIP_2 concentrations and is independent of the presence or absence of the other major uncharged inner leaflet lipid PE.

Synaptotagmin I C2 Domain Binding to Asymmetric Two-Phase Bilayers Composed of Different Concentrations of PS and PE. Figure 4 shows syt I C2A (Figure 4A) and C2AB (Figure 4B) fluorescence intensity ratios of l_o domain regions to l_d nondomain regions after binding to asymmetric two-phase lipid bilayers in the presence of 1 mM Ca^{2+}. All outer leaflets contained bPC and bSM (1:1) with 20% cholesterol. The inner leaflets contained bPC, 15 or 40% POPS, and 20% cholesterol, with or without bPE (1:1 bPC:bPE ratio).

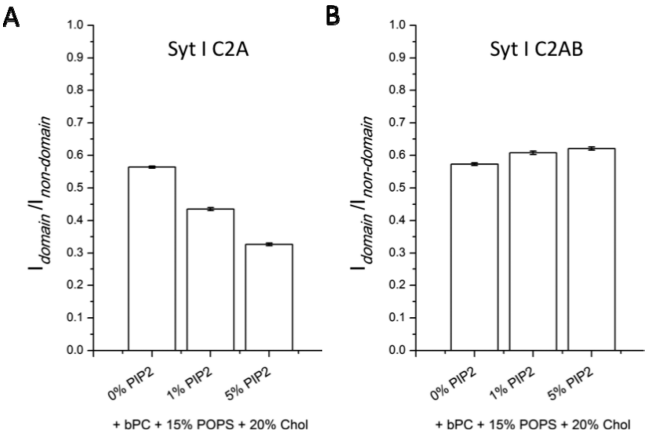

Figure 5. Synaptotagmin I C2A (A) and C2AB (B) fluorescence intensity ratios of ordered lipid domain regions to disordered lipid nondomain regions after binding to asymmetric two-phase bilayers in the presence of 1 mM Ca^{2+} and increasing concentrations of $bPIP_2$ in the inner leaflet monolayers as indicated on the *x*-axis. All outer leaflet monolayers are composed of bPC and bSM (1:1) with 20% cholesterol and supported on a polymer cushion. Error bars indicate standard errors.

No significant differences in the mean intensity ratios were observed after binding of C2A to inner leaflet monolayers containing 15 or 40% PS. The ratios were still close to 0.5, indicating that Ca^{2+}-mediated binding did not redistribute PS between the ordered and disordered phases. Again, twice as much C2A bound to the l_d phase regions as to the l_o phase regions. However, C2AB bound better to l_o phase regions than C2A, and this effect was more pronounced at 40% PS than at 15% PS. The mean fluorescence intensity ratios were 0.59 (15% PS) or 0.71 (40% PS), indicating that compared to C2A more C2AB bound to the l_o phase and that the enhancement of l_d over l_o phase binding of C2AB was only 1.7- and 1.4-fold at 15 and 40% PS, respectively. Adding bPE to inner leaflet monolayers largely reversed this effect and restored the enhancement to ~2-fold. These results suggest that binding of C2AB to ordered regions of PC membranes is enhanced at high PS concentrations compared to binding of C2A. However, this binding enhancement does not take place in equimolar PC/PE membranes with high concentrations of PS. A possible explanation for this effect is that PEs, which have higher chain melting phase transitions than equivalent PCs, do not allow for a similar penetration of C2AB domains in the ordered phase and/or may not allow for protein-induced redistribution of PS in favor of the ordered phase like a PC bilayer does.

Synaptotagmin I C2 Domain Binding to Asymmetric Two-Phase Bilayers Composed of Different Concentrations of PIP_2. In panels C and D of Figure 2, we present images of C2A and C2AB binding to two-phase bilayers containing 1% PIP_2 in addition to 15% PS. Figure 5 shows syt I C2A (Figure 5A) and C2AB (Figure 5B) fluorescence intensity ratios of l_o domain regions to l_d nondomain regions after binding to asymmetric two-phase lipid bilayers in the presence of 1 mM Ca^{2+} with various amounts of PIP_2 included. All the outer leaflets contained bPC and bSM (1:1) with 20% cholesterol, while the inner leaflets contained bPC, 15% POPS, 20% cholesterol, and 0−5% $bPIP_2$. Compared to the PS-containing bilayers without PIP_2, the l_o−l_d phase partitioning of C2A shifted by ~20%, and 40% less C2A bound to the l_o phase regions when 1 or 5% PIP_2 was added. At 1% PIP_2, C2A is up to 2.3 times more likely to be found in the l_d phase than in the l_o phase, but at 5% PIP_2, this factor increases to 3.1. Because we have already established with C2AB binding to these membranes in the absence of Ca^{2+} that the balance of PS and PIP_2 partitioning between the l_o and l_d phases is independent of the PIP_2 concentration (Figure 3B), the enhanced binding of C2A is most likely due to more C2A binding to the higher concentrations of PIP_2 present in the l_d phase than in the l_o phase. Moreover, even more PIP_2 may accumulate in the l_d phase as a result of protein binding and could additionally contribute to the increased level of binding to this phase. Interestingly, the level of C2AB binding to the l_o phase regions increased by 6−7% when 1 or 5% PIP_2 was added. As was the case with PS, C2AB in the presence of Ca^{2+} seems to have a higher affinity for l_o phases than C2A and therefore may tip the balance to more PIP_2 partitioning into l_o phases than is the case after C2A binding to phase-separated lipid membranes with the same compositions.

DISCUSSION

Eighty-five years ago, Gorter and Grendel discovered in pioneering work that biological membranes are formed by lipid bilayers.[40] Forty-seven years later, Singer and Nicolson introduced the "fluid mosaic model", in which the plasma membrane is regarded as a two-dimensional solution of freely diffusing membrane proteins embedded in a fluid lipid bilayer.[41] In this model, the bilayer is considered to be a uniform, semipermeable barrier that serves as a passive homogeneous fluid matrix for membrane proteins. However, after extensive research on the dynamics and organization of plasma and organellar membranes, biological membranes are now considered to be much more organized and laterally heterogeneous than previously thought. A popular explanation for this inhomogeneity is the existence of lipid micro- or nanodomains in cellular membranes that are sometimes also termed lipid "rafts".[42,43] The physical properties and biological functions of these domains have received significant attention over the past 15 years. Lipid rafts have been equated with detergent-resistant biochemical membrane fractions (DRMs) and have been proposed to be involved in a wide variety of important cellular processes, particularly in signal transduction, membrane protein sorting, membrane trafficking, and the budding of viral particles from cell surfaces.[44]

More than 200 membrane proteins have been found in DRMs,[45] and various SNARE proteins have been included in this list.[46,47] However, other interpretations of cholesterol-dependent cluster formation of SNAREs have been proposed.[28,29,48] When SNAREs were reconstituted in coexisting l_o and l_d phase giant unilamellar vesicles, they partitioned favorably into the l_d phase regions.[49] Therefore, it appears that SNAREs may actually be excluded from cholesterol-rich membrane regions. SNAREs and synaptotagmin I are cooperating in Ca^{2+}-regulated membrane fusion in neurosecretion. Following the commonly accepted model that syt I functions by binding at least with its C2B domain to the presynaptic membrane, it may be efficient to target its C2 domains to the same membrane domains as the SNAREs at nascent fusion sites at the synapse. Because the synaptic vesicle protein syt I interacts via one or both of its C2 domains only with the cytoplasmic leaflets of the presynaptic plasma or vesicle membranes, it does not encounter lipid mixtures that form large rafts in vitro (PC, SM, and cholesterol), because these lipids are mostly localized in the outer leaflets of plasma membranes.[50] As shown in this study, C2 domains indeed interact preferentially with the more disordered (nonraft) inner leaflet regions of asymmetric

lipid model membranes. Therefore, they are targeted to the same regions of the membrane as SNAREs, thereby enhancing the likelihood that these molecules are colocalized and act together in the cell.

To the best of our knowledge, this is the first time that the l_o and l_d phase domain targeting of an electrostatically bound and partially membrane-penetrating membrane protein has been studied on an inner leaflet raft lipid mixture. The method should of course be valid for studying the targeting of many other peripheral inner leaflet membrane proteins. A plethora of intracellular signaling domains interact with plasma membranes in this fashion, and it will be very interesting to see how they partition between different lipid phases and whether they actually fulfill a central tenet of the raft hypothesis of transmembrane signal transduction, which is that they should copartition into the same lipid domains of the plasma membrane as extracellular receptors after stimulation with appropriate ligands.

The supported asymmetric two-phase lipid bilayer system[30,32] that we used here has several advantages that make it attractive for these studies. First, the bilayers have asymmetric lipid distributions, which closely mimic those in plasma membranes and which are difficult to achieve in other model membrane systems. The major lipid components from outer (PC, SM, and cholesterol) and inner (PC, PE, PS, PI, and cholesterol) leaflets of plasma membranes can be used pretty much at will to form the first and second monolayers of the supported bilayers, respectively. We have discovered previously that coexisting l_o and l_d phases in outer leaflet lipid mixtures can induce the l_o−l_d phase separation in adjacent inner leaflet lipids by transbilayer phase coupling.[30,32] Second, by changing the inner leaflet lipid compositions in the regions of coexisting l_o and l_d phases as done in this study, we can separate protein−lipid interactions that are lipid-specific (e.g., interactions with a specific acidic lipid) from those that are lipid phase-specific. Of course, these two types of interactions are not always independent, which has been the case with the C2 domains studied here, but at least the interactions can be studied separately in the two coexisting phases. Most bulk methods that are currently in use cannot make this distinction. Third, the planar geometry of supported bilayers facilitates microscopic observations and interpretation of the images because no curvature effects need to be considered.

As with every new method, there are of course also disadvantages. Questions about whether the solid support has any influence on the phase behavior of the supported bilayer persist. We tried to minimize this influence by using a 4 nm polymer cushion between the solid support and bilayer.[51] Despite this cushion, which allows for free diffusion of the lipids and some proteins in both leaflets of the bilayer, the domains as a whole are not moving in this system. They are probably "pinned" in a few places to protrusions or other imperfections on the solid support. Thus, even though we believe that the support−membrane interactions are quite minimal, they are not completely eliminated in this system. Despite this caveat, the exposed inner leaflet surface may not be significantly perturbed by this pinning. Studies with free-standing asymmetric two-phase bilayers in "black lipid membranes" also have found phase coupling between l_o and l_d phase regions across the midplane of the bilayer,[52] i.e., confirming conclusions drawn from our supported membrane approach. No inner leaflet protein targeting experiments have yet been reported in black lipid membranes. Asymmetric membranes may also be produced by lipid exchange in relatively small unilamellar vesicles.[53] However, these vesicles are too small to optically resolve possible phase separations and therefore are not suitable for studying localized membrane protein targeting as conducted here.

In this study, we have focused on binding ratios between l_o and l_d phase regions. We also attempted to obtain absolute binding to individual domain regions in the course of these studies but found this to be more difficult. Absolute fluorescence intensities are not well-calibrated on a TIRF microscope, which makes it difficult to compare experiments performed on different bilayers and different days. There may be ways to remedy this problem with appropriate internal standards in the future, but differences that we observed in individual binding behaviors require careful analysis and confirmation.

Because we observe similar results for binding of C2AB to PS-containing membranes in the absence of Ca^{2+} and C2A in the presence of Ca^{2+}, we think that the PS distribution between these two phases dominates the binding reaction and that these proteins under these conditions may be good reporters of PS partitioning between the two phases. C2AB binding in the absence of Ca^{2+} may be particularly suitable for this purpose because its binding is thought to be purely electrostatic and is not confounded with penetration of the loop into hydrophobic portions of the bilayer.[21] It will be interesting to see whether this method can be further developed in the future as a reliable probe of acidic lipid partitioning between different lipid phases. More systematic studies along these lines and a more thorough analysis in terms of the electrostatic surface potential on binding will be required to further develop this method into a truly quantitative tool for measuring acidic lipid partitioning.

Our result that C2A binds in the presence of Ca^{2+} very strongly to PIP_2 in the l_d phase is not surprising. Brain PIP_2 has highly unsaturated acyl chains and therefore likely partitions well into the l_d phase. Because PIP_2 bears a negative charge of −3 to −4 at neutral pH, it is expected to strongly electrostatically attract Ca^{2+}-bound C2A. C2A also partially penetrates into the hydrophobic interior of the bilayer, which should be facilitated by the more disordered l_d phase compared to the more ordered l_o phase. These two factors may cooperate as the overall PIP_2 concentration is increased in the membrane and thereby further shift this lipid's partition equilibrium to the l_d phase at high PIP_2 concentrations. Interestingly, this cooperative effect is not observed with C2AB. C2AB clearly has a higher affinity for the l_o phase than C2A. The opposing forces of greater PIP_2 partitioning into the l_d phase and the higher relative affinity of C2AB toward the l_o phase probably cancel the fluidity−electrostatic cooperativity that has been seen with C2A and could explain the observed difference between the behaviors of C2A and C2AB in these lipid systems.

In summary, this study of acidic lipid targeting of synaptotagmin I C2 domains to membrane regions of different lipid acyl chain order provided fundamental new insight into how acidic lipids are distributed between ordered and disordered regions of the inner leaflet in heterogeneous asymmetric lipid bilayers. It also provided fundamental new information about how synaptotagmin I may target heterogeneously structured lipid surfaces of plasma membranes from a position within cells. Importantly, syt I and PIP_2 appear to be targeted to membrane regions similar to those to which SNAREs are targeted. This should increase the probability of encounter and functional interaction of SNAREs, syt I, PIP_2, and Ca^{2+} in these regions. The membrane therefore likely acts as an organizing medium, bringing several of the most critical components together, which are all known players in

Ca^{2+}-triggered exocytosis by membrane fusion in neuroendocrine cells. This principle of organizing functionally related membrane components in similar locations in the membrane may not be limited to membrane fusion but could also operate in other membrane-assembled molecular machines or membrane-assisted systems of signal transduction.

■ ASSOCIATED CONTENT

Supporting Information. One figure demonstrating the coupling of lipid phases between outer and inner leaflets in two-phase lipid bilayers. This material is available free of charge via the Internet at http://pubs.acs.org.

■ AUTHOR INFORMATION

Corresponding Author

*Phone: (434) 982-3578. Fax: (434) 243-8271. E-mail: lkt2e@virginia.edu.

Notes

[a]C2 domain binding data similar to those presented throughout this study were also obtained with bPS instead of POPS, but the results were generally more consistent with POPS (smaller standard errors) than with bPS in the inner leaflets (data not shown). Generally, the same conclusions can be drawn with both lipids.

Funding Sources

This work was supported by National Institutes of Health Grant P01 GM072694.

■ ACKNOWLEDGMENT

We thank Dr. Michael Wiener for his interest and helpful comments in the course of this work. We also thank members of the Tamm laboratory for many helpful discussions.

■ ABBREVIATIONS

bPC, porcine brain phosphatidylcholine; bSM, porcine brain sphingomyelin; bPE, porcine brain phosphatidylethanolamine; $bPIP_2$, brain phosphatidylinositol 4,5-bisphosphate; Chol, cholesterol; DPS, 1,2-dimyristoylphosphatidylethanolamine-*N*-[poly(ethylene glycol)triethoxysilane]; EGTA, ethylene glycol bis(β-aminoethylether) *N*,*N*′-tetraacetic acid; NBD-DPPE, 1,2-dipalmitoylphosphatidylethanolamine-*N*-(7-nitro-2-1,3-benzoxadiazol-4-yl); POPS, 1-palmitoyl-2-oleoylphosphatidylserine; Rh-DPPE, 1,2-dipalmitoylphosphatidylethanolamine-*N*-(lissamine rhodamine B sulfonyl); syt I, synaptotagmin I; syt I C2AB, soluble fragment of synaptotagmin I containing the C2A and C2B domains; syt I C2A, C2A domain of syt I; syt I C2B, C2B domain of syt I; SNARE, soluble *N*-ethylmaleimide-sensitive factor attachment receptor; SNAP-25, synaptosomal-associated protein of 25 kDa; TIRFM, total internal reflection fluorescence microscopy; TM, transmembrane.

■ REFERENCES

(1) Jahn, R., Lang, T., and Sudhof, T. C. (2003) Membrane fusion. *Cell 112*, 519–533.

(2) Rizo, J., and Rosenmund, C. (2008) Synaptic vesicle fusion. *Nat. Struct. Mol. Biol. 15*, 665–674.

(3) Sudhof, T. C., and Rothman, J. E. (2009) Membrane fusion: Grappling with SNARE and SM proteins. *Science 323*, 474–477.

(4) Brunger, A. T. (2005) Structure and function of SNARE and SNARE-interacting proteins. *Q. Rev. Biophys. 38*, 1–47.

(5) Fasshauer, D. (2003) Structural insights into the SNARE mechanism. *Biochim. Biophys. Acta 1641*, 87–97.

(6) Jahn, R., and Scheller, R. H. (2006) SNAREs: Engines for membrane fusion. *Nat. Rev. Mol. Cell Biol. 7*, 631–643.

(7) McNew, J. A. (2008) Regulation of SNARE-mediated membrane fusion during exocytosis. *Chem. Rev. 108*, 1669–1686.

(8) Sollner, T. H. (2003) Regulated exocytosis and SNARE function (Review). *Mol. Membr. Biol. 20*, 209–220.

(9) Brose, N., Petrenko, A. G., Sudhof, T. C., and Jahn, R. (1992) Synaptotagmin: A calcium sensor on the synaptic vesicle surface. *Science 256*, 1021–1025.

(10) Chapman, E. R. (2008) How does synaptotagmin trigger neurotransmitter release?. *Annu. Rev. Biochem. 77*, 615–641.

(11) Fernandez-Chacon, R., Konigstorfer, A., Gerber, S. H., Garcia, J., Matos, M. F., Stevens, C. F., Brose, N., Rizo, J., Rosenmund, C., and Sudhof, T. C. (2001) Synaptotagmin I functions as a calcium regulator of release probability. *Nature 410*, 41–49.

(12) Jackson, M. B., and Chapman, E. R. (2006) Fusion pores and fusion machines in Ca^{2+}-triggered exocytosis. *Annu. Rev. Biophys. Biomol. Struct. 35*, 135–160.

(13) Perin, M. S., Fried, V. A., Mignery, G. A., Jahn, R., and Sudhof, T. C. (1990) Phospholipid binding by a synaptic vesicle protein homologous to the regulatory region of protein kinase C. *Nature 345*, 260–263.

(14) Perin, M. S., Brose, N., Jahn, R., and Sudhof, T. C. (1991) Domain structure of synaptotagmin (p65). *J. Biol. Chem. 266*, 623–629.

(15) Fernandez, I., Arac, D., Ubach, J., Gerber, S. H., Shin, O., Gao, Y., Anderson, R. G., Sudhof, T. C., and Rizo, J. (2001) Three-dimensional structure of the synaptotagmin 1 C2B-domain: Synaptotagmin 1 as a phospholipid binding machine. *Neuron 32*, 1057–1069.

(16) Ubach, J., Zhang, X., Shao, X., Sudhof, T. C., and Rizo, J. (1998) Ca^{2+} binding to synaptotagmin: How many Ca^{2+} ions bind to the tip of a C2-domain?. *EMBO J. 17*, 3921–3930.

(17) Martens, S., and McMahon, H. T. (2008) Mechanisms of membrane fusion: Disparate players and common principles. *Nat. Rev. Mol. Cell Biol. 9*, 543–556.

(18) Chapman, E. R., and Davis, A. F. (1998) Direct interaction of a Ca^{2+}-binding loop of synaptotagmin with lipid bilayers. *J. Biol. Chem. 273*, 13995–14001.

(19) Herrick, D. Z., Sterbling, S., Rasch, K. A., Hinderliter, A., and Cafiso, D. S. (2006) Position of synaptotagmin I at the membrane interface: Cooperative interactions of tandem C2 domains. *Biochemistry 45*, 9668–9674.

(20) Rufener, E., Frazier, A. A., Wieser, C. M., Hinderliter, A., and Cafiso, D. S. (2005) Membrane-bound orientation and position of the synaptotagmin C2B domain determined by site-directed spin labeling. *Biochemistry 44*, 18–28.

(21) Kuo, W., Herrick, D. Z., Ellena, J. F., and Cafiso, D. S. (2009) The calcium-dependent and calcium-independent membrane binding of synaptotagmin 1: Two modes of C2B binding. *J. Mol. Biol. 387*, 284–294.

(22) Bai, J., Tucker, W. C., and Chapman, E. R. (2004) PIP2 increases the speed of response of synaptotagmin and steers its membrane-penetration activity toward the plasma membrane. *Nat. Struct. Mol. Biol. 11*, 36–44.

(23) Bai, J., Wang, P., and Chapman, E. R. (2002) C2A activates a cryptic Ca^{2+}-triggered membrane penetration activity within the C2B domain of synaptotagmin I. *Proc. Natl. Acad. Sci. U.S.A. 99*, 1665–1670.

(24) Cafiso, D. S. (2005) *Structure and Interactions of C2 Domains at Membrane Surfaces*, Wiley-VCH, Weinheim, Germany.

(25) Martens, S., Kozlov, M. M., and McMahon, H. T. (2007) How synaptotagmin promotes membrane fusion. *Science 316*, 1205–1208.

(26) Lee, H. K., Yang, Y., Su, Z., Hyeon, C., Lee, T. S., Lee, H. W., Kweon, D. H., Shin, Y. K., and Yoon, T. Y. (2010) Dynamic Ca^{2+}-

dependent stimulation of vesicle fusion by membrane-anchored synaptotagmin 1. *Science 328*, 760–763.

(27) Stein, A., Radhakrishnan, A., Riedel, D., Fasshauer, D., and Jahn, R. (2007) Synaptotagmin activates membrane fusion through a Ca^{2+}-dependent trans interaction with phospholipids. *Nat. Struct. Mol. Biol. 14*, 904–911.

(28) Lang, T., Bruns, D., Wenzel, D., Riedel, D., Holroyd, P., Thiele, C., and Jahn, R. (2001) SNAREs are concentrated in cholesterol-dependent clusters that define docking and fusion sites for exocytosis. *EMBO J. 20*, 2202–2213.

(29) Ohara-Imaizumi, M., Nishiwaki, C., Kikuta, T., Kumakura, K., Nakamichi, Y., and Nagamatsu, S. (2004) Site of docking and fusion of insulin secretory granules in live MIN6 β cells analyzed by TAT-conjugated anti-syntaxin 1 antibody and total internal reflection fluorescence microscopy. *J. Biol. Chem. 279*, 8403–8408.

(30) Wan, C., Kiessling, V., and Tamm, L. K. (2008) Coupling of cholesterol-rich lipid phases in asymmetric bilayers. *Biochemistry 47*, 2190–2198.

(31) Wang, T. Y., and Silvius, J. R. (2001) Cholesterol does not induce segregation of liquid-ordered domains in bilayers modeling the inner leaflet of the plasma membrane. *Biophys. J. 81*, 2762–2773.

(32) Kiessling, V., Crane, J. M., and Tamm, L. K. (2006) Transbilayer effects of raft-like lipid domains in asymmetric planar bilayers measured by single molecule tracking. *Biophys. J. 91*, 3313–3326.

(33) Frazier, A. A., Roller, C. R., Havelka, J. J., Hinderliter, A., and Cafiso, D. S. (2003) Membrane-bound orientation and position of the synaptotagmin I C2A domain by site-directed spin labeling. *Biochemistry 42*, 96–105.

(34) Crane, J. M., Kiessling, V., and Tamm, L. K. (2005) Measuring lipid asymmetry in planar supported bilayers by fluorescence interference contrast microscopy. *Langmuir 21*, 1377–1388.

(35) Kalb, E., Frey, S., and Tamm, L. K. (1992) Formation of supported planar bilayers by fusion of vesicles to supported phospholipid monolayers. *Biochim. Biophys. Acta 1103*, 307–316.

(36) Wagner, M. L., and Tamm, L. K. (2000) Tethered polymer-supported planar lipid bilayers for reconstitution of integral membrane proteins: Silane-polyethyleneglycol-lipid as a cushion and covalent linker. *Biophys. J. 79*, 1400–1414.

(37) Oreopoulos, J., and Yip, C. M. (2009) Combinatorial microscopy for the study of protein-membrane interactions in supported lipid bilayers: Order parameter measurements by combined polarized TIRFM/AFM. *J. Struct. Biol. 168*, 21–36.

(38) Kiessling, V., Domanska, M. K., and Tamm, L. K. (2010) Single SNARE-mediated vesicle fusion observed in vitro by polarized TIRFM. *Biophys. J. 99*, 4047–4055.

(39) Crane, J. M., and Tamm, L. K. (2004) Role of cholesterol in the formation and nature of lipid rafts in planar and spherical model membranes. *Biophys. J. 86*, 2965–2979.

(40) Gorter, E., and Grendel, F. (1925) On Bimolecular Layers of Lipoids on the Chromocytes of the Blood. *J. Exp. Med. 41*, 439–443.

(41) Singer, S. J., and Nicolson, G. L. (1972) The fluid mosaic model of the structure of cell membranes. *Science 175*, 720–731.

(42) London, E. (2005) How principles of domain formation in model membranes may explain ambiguities concerning lipid raft formation in cells. *Biochim. Biophys. Acta 1746*, 203–220.

(43) Simons, K., and Ikonen, E. (1997) Functional rafts in cell membranes. *Nature 387*, 569–572.

(44) Lingwood, D., and Simons, K. (2010) Lipid rafts as a membrane-organizing principle. *Science 327*, 46–50.

(45) Foster, L. J., De Hoog, C. L., and Mann, M. (2003) Unbiased quantitative proteomics of lipid rafts reveals high specificity for signaling factors. *Proc. Natl. Acad. Sci. U.S.A. 100*, 5813–5818.

(46) Chamberlain, L. H., Burgoyne, R. D., and Gould, G. W. (2001) SNARE proteins are highly enriched in lipid rafts in PC12 cells: Implications for the spatial control of exocytosis. *Proc. Natl. Acad. Sci. U.S.A. 98*, 5619–5624.

(47) Salaun, C., Gould, G. W., and Chamberlain, L. H. (2005) Lipid raft association of SNARE proteins regulates exocytosis in PC12 cells. *J. Biol. Chem. 280*, 19449–19453.

(48) Murray, D. H., and Tamm, L. K. (2009) Clustering of syntaxin-1A in model membranes is modulated by phosphatidylinositol 4,5-bisphosphate and cholesterol. *Biochemistry 48*, 4617–4625.

(49) Bacia, K., Schuette, C. G., Kahya, N., Jahn, R., and Schwille, P. (2004) SNAREs prefer liquid-disordered over "raft" (liquid-ordered) domains when reconstituted into giant unilamellar vesicles. *J. Biol. Chem. 279*, 37951–37955.

(50) Kiessling, V., Wan, C., and Tamm, L. K. (2009) Domain coupling in asymmetric lipid bilayers. *Biochim. Biophys. Acta 1788*, 64–71.

(51) Kiessling, V., and Tamm, L. K. (2003) Measuring distances in supported bilayers by fluorescence interference-contrast microscopy: Polymer supports and SNARE proteins. *Biophys. J. 84*, 408–418.

(52) Collins, M. D., and Keller, S. L. (2008) Tuning lipid mixtures to induce or suppress domain formation across leaflets of unsupported asymmetric bilayers. *Proc. Natl. Acad. Sci. U.S.A. 105*, 124–128.

(53) Cheng, H. T., Megha, and London, E. (2009) Preparation and properties of asymmetric vesicles that mimic cell membranes: Effect upon lipid raft formation and transmembrane helix orientation. *J. Biol. Chem. 284*, 6079–6092.